

# Unmixing highly mixed grain size distribution data via maximum volume constrained end member analysis

Qianqian Qi

Hangzhou Dianzi University, China  
[q.qi@hdu.edu.cn](mailto:q.qi@hdu.edu.cn)

Zhongming Chen

Hangzhou Dianzi University, China  
[zmchen@hdu.edu.cn](mailto:zmchen@hdu.edu.cn)

Peter G. M. van der Heijden

Utrecht University, the Netherlands and University of Southampton, UK  
[p.g.m.vanderheijsden@uu.nl](mailto:p.g.m.vanderheijsden@uu.nl)

## Abstract

End member analysis (EMA) unmixes grain size distribution (GSD) data into a mixture of end members (EMs), thus helping understand sediment provenance and depositional regimes and processes. In highly mixed data sets, however, many EMA algorithms find EMs which are still a mixture of true EMs. To overcome this, we propose maximum volume constrained EMA (MVC-EMA), which finds EMs as different as possible. We provide a uniqueness theorem and a quadratic programming algorithm for MVC-EMA. Experimental results show that MVC-EMA can effectively find true EMs in highly mixed data sets.

**Keywords:** Nonnegative matrix analysis; Minimum volume; Identifiability; Sufficient scattered conditions.

## 1 Introduction

In sedimentary geology, unmixing grain size distribution (GSD) data into a mixture of end members (EMs), called end member analysis (EMA), can help understand sediment provenance and depositional regimes and processes (Lin et al., 2025; Liu et al., 2023; Moskalewicz & Winter, 2024; Paterson & Heslop, 2015; Renner, 1995; Renny et al., 2026; Van Hateren, Prins, & Van Balen, 2018; Weltje, 1997). Denote  $\mathbf{P}$  as a data matrix of size  $I \times J$ . Each row of  $\mathbf{P}$  represents an observed specimen of GSD data with nonnegative and sum-to-1 constraints:  $\mathbf{P} \geq 0$  and  $\mathbf{P}\mathbf{1} = \mathbf{1}$ , where  $\geq$  means that each elements in the matrix is non-negative and  $\mathbf{1}$  is the vector of all ones of appropriate dimension. EMA approximates a GSD data  $\mathbf{P}$  by a lower rank matrix  $\mathbf{\Pi}$  which is the product of two nonnegative matrices with row-sum-to-1 constraint. Thus, EMA can be expressed as

$$\begin{aligned} \min \quad & \frac{1}{2} \|\mathbf{P} - \mathbf{\Pi}\|_F^2 \\ \text{subject to} \quad & \mathbf{\Pi} = \mathbf{W}\mathbf{G}, \quad \mathbf{W}\mathbf{1} = \mathbf{1}, \quad \mathbf{G}\mathbf{1} = \mathbf{1} \\ & \mathbf{W} \in \mathbb{R}_+^{I \times K}, \quad \mathbf{G} \in \mathbb{R}_+^{K \times J} \end{aligned} \tag{1}$$

where  $K \leq \min\{I, J\}$  and the Frobenius norm of a matrix  $\mathbf{A}$  is defined by  $\|\mathbf{A}\|_F^2 = \sqrt{\sum_i \sum_j \mathbf{A}(i, j)^2}$ . In addition to Frobenius norm, there are other objective function such as  $L_1$  norm to measure the discrepancy between  $\mathbf{P}$  and  $\mathbf{\Pi}$  (Zhang, Wang, Xu, & Yang, 2020). Each row of  $\mathbf{G}$  is a end-member, and each specimen in  $\mathbf{\Pi}$  is constructed by these end-members with weights or abundances in the corresponding row of  $\mathbf{W}$ .  $\mathbf{W}$  and  $\mathbf{G}$  are called the abundance matrix and the end-member matrix, respectively. Geometrically, the rows of  $\mathbf{\Pi}$  are in the convex hull generated by the rows of  $\mathbf{G}$  (Avis & Bremner, 1995; Gillis,

2020). Given an observed matrix  $\mathbf{P}$ , EMA aims to recover  $\mathbf{W}$  and  $\mathbf{G}$  that yield the lower rank matrix  $\mathbf{\Pi}$ .

EMA, however, is not unique (Paterson & Heslop, 2015; Renner, 1993, 1995; Weltje, 1997; Weltje & Prins, 2007; Zhang et al., 2020). Given EMA  $\mathbf{\Pi} = \mathbf{WG}$ , we have

$$\mathbf{\Pi} = \mathbf{WUU}^{-1}\mathbf{G},$$

where  $\mathbf{U}$  is a full rank matrix of size  $K \times K$ . The sum-to-one conditions  $\mathbf{WU}\mathbf{1} = \mathbf{1}$  and  $\mathbf{U}^{-1}\mathbf{G}\mathbf{1} = \mathbf{1}$  hold if and only if  $\mathbf{U}\mathbf{1} = \mathbf{1}$  (De Leeuw, Van der Heijden, & Verboon, 1990). The nonnegativity constraints  $\mathbf{WU} \geq 0$  and  $\mathbf{U}^{-1}\mathbf{G} \geq 0$  further restrict the admissible set of  $\mathbf{U}$ . However, even under these constraints,  $\mathbf{U}$  may be more than permutation, implying that EMA admits multiple equivalent solutions of the form  $(\mathbf{WU}, \mathbf{U}^{-1}\mathbf{G})$ . Geometrically, nonuniqueness can be understood as that any convex hull enclosing all data points could be solutions of EMA.

Many EMA algorithms choose to identify the solution by using minimum EMs, i.e. EMs that enclose specimens as tightly as possible (Dietze, Schulte, & Dietze, 2022; Paterson & Heslop, 2015; Van Hateren et al., 2018; Weltje, 1997; Weltje & Prins, 2007). However, this framework fails for highly mixed data where no single specimen is near a true end-member. This is because estimated EMs are themselves mixtures of the true EMs. Highly mixed data, however, are common in natural settings. Following Paterson and Heslop (2015), we illustrate a highly mixed case using a simulated GSD data ( $99 \times 100$ ). The data are derived from two lognormal EMs, with abundances always not less than 0.13 (Figure 1a, 1b). Applying end member modelling algorithm (EMMA) (Seidel & Hlawitschka, 2015; Weltje, 1997), a fundamental minimum-EMs algorithm, produces two bimodal EMs (Figure 1c). Each EM is dominated by a source but is contaminated by the other, leading to abundance misestimation (Figure 1d).

The "outermost EMs" concept was proposed for highly mixed data by Zhang et al. (2020), analogous to the "outer extreme solution" in latent budget analysis (LBA) (Van der Ark, Van der Heijden, & Sikkel, 1999). Notably, LBA has the same parametric form  $\mathbf{\Pi} = \mathbf{WG}$  as EMA (Clogg, 1981; De Leeuw et al., 1990; Van der Heijden, 1994). LBA was developed in the social sciences which can explain pattern of time allocation. However, the framework "outermost EMs" or "outer extreme solution" lacks uniqueness theorems. The only known uniqueness condition, from De Leeuw et al. (1990), is limited to dimensionality  $K = 2$ , while  $K > 2$  regularly happens in practice. On the algorithmic side, to find outermost EMs, Zhang et al. (2020) make use of a genetic algorithm. The genetic algorithm is an flexible and widely used algorithm, inspired by natural selection mechanisms. However, due to its stochastic and heuristic nature, it has no guarantee to obtain the global optima and even local optima. Van der Ark et al. (1999) proposed Metropolis algorithm to seek the outer extreme solution (Jelihovschi & Allaman, 2018). Likewise, the Metropolis algorithm is heuristic in nature.

The "outermost EMs" or "outer extreme solution" is defined in terms of the maximum of the sum of distances between EMs such as the sum of Manhattan or of chi-squared

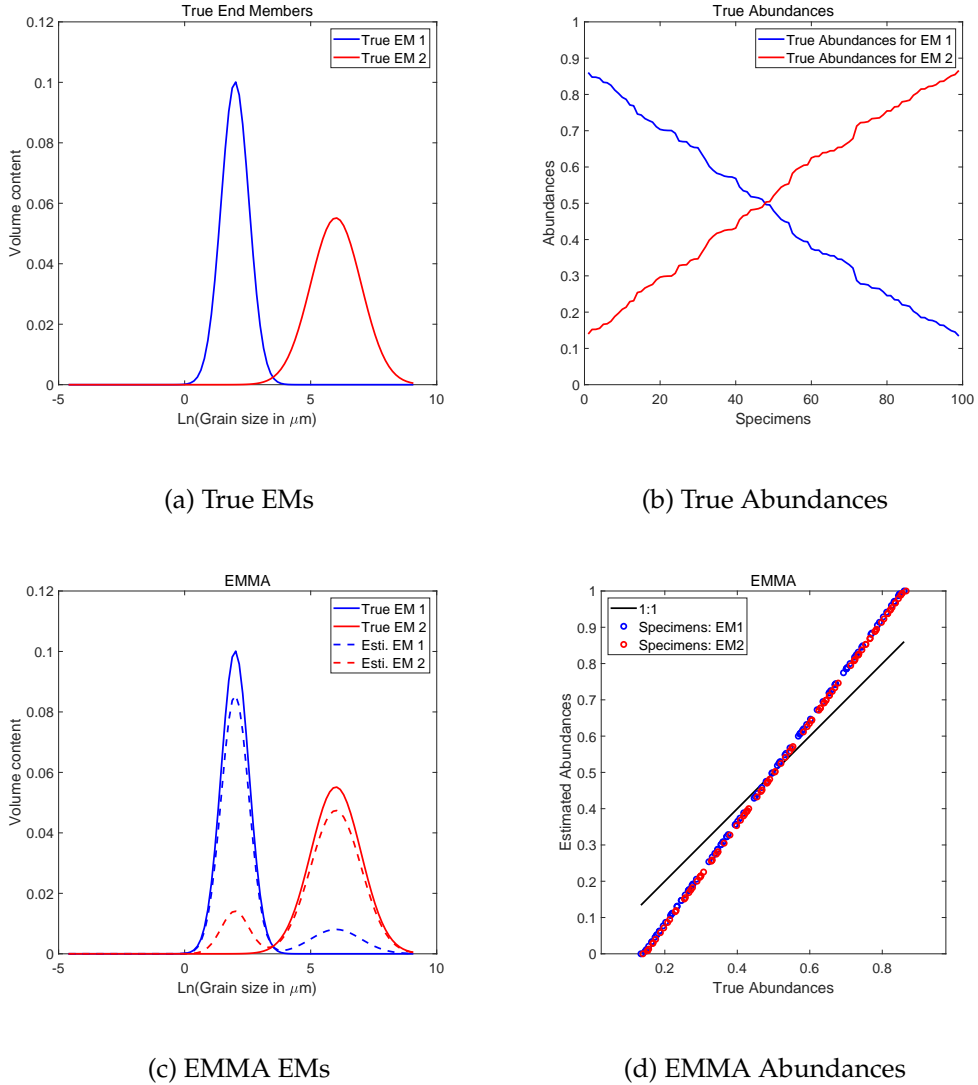


Figure 1: (a and b) Two lognormal EMs and their abundances; (c and d) EMMA unmixing results.

distances (Van der Ark et al., 1999; Zhang et al., 2020). In contrast, the minimum volume assumption - closely related to "minimum EMs" - has been studied intensively in nonnegative matrix factorization (NMF), that decomposes a nonnegative matrix into the product of two nonnegative matrices, and that includes EMA as a special case (Fu, Huang, Sidiropoulos, & Ma, 2019; Gillis, 2020; Guo, Li, & Liang, 2024; Hobolth, Guo, Kousholt, & Jensen, 2020; Lee & Seung, 1999; Paatero & Tapper, 1994; Qi & Van der Heijden, 2025; Saberi-Movahed et al., 2025). NMF using the minimum volume assumption has been studied in considerable detail for uniqueness theorems and algorithms, which, partly, benefits from the fact that the volume measure is related to the determinant of  $GG^T$  rather than related to distances (Abdolali, Barbarino, & Gillis, 2024; Fu, Huang, & Sidiropoulos, 2018; Fu, Ma, Huang, & Sidiropoulos, 2015; Guo et al., 2024; Hobolth et al., 2020; Leplat, Gillis, & Ang, 2020; Lin, Ma, Li, Chi, & Ambikapathi, 2015; Saberi-Movahed et al., 2025).

According to [Fu et al. \(2019\)](#); [Fu, Huang, Yang, Ma, and Sidiropoulos \(2016\)](#), the sum of squared distances between all the pairs of basis vectors  $\mathbf{G}$  is an approximation of the volume of basis matrix  $\mathbf{G}$ . In the simulation part of the paper by [Fu et al. \(2016\)](#), the regularizer related to the sum of squared distances between basis vectors is slightly worse than the regularizer related to the volume of basis matrix  $\mathbf{G}$  in terms of the mean-squared-error (MSE) of abundance. However, to the best of knowledge, a volume regularizer has never been used in EMA before.

Motivated by these insights, we propose maximum volume constrained end member analysis (MVC-EMA) for highly mixed data. Section 2 proposes a sufficient condition for MVC-EMA to be unique. Section 3 proposes an algorithm, named APFGM short for alternative projected fast gradient methods. This algorithm can perform minimum, no, and maximum volume assumptions. Section 4 compares APFGM with maximum volume, APFGM with no volume, APFGM with minimum volume, and EMMA (a classic algorithm for "Minimum EMs" in sedimentary geology). Finally, Section 5 concludes this paper.

## 2 Uniqueness theorem under the maximum volume assumption

Before beginning this section, we introduce two lemmas in linear algebra, which are used later in this section ([Gillis, 2020](#)). The cone of a matrix  $\mathbf{A} \in \mathbb{R}^{I \times J}$  is defined by

$$\text{cone}(\mathbf{A}) = \left\{ \sum_j r_j \mathbf{A}(:, j) \mid r_j \geq 0, j = 1, \dots, J \right\}.$$

**Lemma 1.** *Given a matrix  $\mathbf{A}$ , the dual of  $\text{cone}(\mathbf{A})$  is defined by  $\text{cone}^*(\mathbf{A}) = \{\mathbf{y} \mid \mathbf{A}^T \mathbf{y} \geq 0\}$ .*

**Lemma 2.** *Given two matrices  $\mathbf{A}$  and  $\mathbf{B}$ , if  $\text{cone}(\mathbf{A}) \subseteq \text{cone}(\mathbf{B})$ , then  $\text{cone}^*(\mathbf{B}) \subseteq \text{cone}^*(\mathbf{A})$ .*

**Definition 1.** *The EMA solution  $(\mathbf{W}, \mathbf{G})$  of  $\mathbf{\Pi}$  is said to be essentially unique if and only if any other EMA solution  $(\tilde{\mathbf{W}}, \tilde{\mathbf{G}})$  has the form*

$$\tilde{\mathbf{W}} = \mathbf{W}\mathbf{\Gamma}^{-1} \text{ and } \tilde{\mathbf{G}} = \mathbf{\Gamma}\mathbf{G}$$

where  $\mathbf{\Gamma}$  is a permutation matrix.

Given the lower rank matrix  $\mathbf{\Pi} \in \mathbb{R}_+^{I \times J}$  with  $\mathbf{\Pi}\mathbf{1} = \mathbf{1}$ , one wants to find an essentially unique solution of EMA  $\mathbf{\Pi} = \mathbf{W}\mathbf{G}$  under the assumption of maximum volume. Formally, the maximum volume constrained end member analysis (MVC-EMA) is formulated as follows:

$$\begin{aligned} & \max \quad \det(\mathbf{G}\mathbf{G}^T) \\ & \text{subject to} \quad \mathbf{\Pi} = \mathbf{W}\mathbf{G}, \quad \mathbf{W}\mathbf{1} = \mathbf{1}, \quad \mathbf{G}\mathbf{1} = \mathbf{1} \\ & \quad \mathbf{W} \in \mathbb{R}_+^{I \times K}, \quad \mathbf{G} \in \mathbb{R}_+^{K \times J} \end{aligned} \tag{2}$$

where  $K \leq \min\{I, J\}$  and  $\det(\mathbf{G}\mathbf{G}^T)$  refers to the determinant of  $\mathbf{G}\mathbf{G}^T$ .

A sufficiently scattered condition (SSC) is a sufficient condition for minimum volume constrained nonnegative matrix factorization (NMF) to be unique (Fu et al., 2018, 2015; Leplat et al., 2020). In minimum volume constrained NMF, SSC is used in the context of the coefficient matrix/abundance matrix. Here, we introduce SSC to MVC-EMA. In contrast to minimum volume constrained NMF, SSC is used in the context of the basis matrix/end-member matrix in MVC-EMA. SSC is related to sparsity. This implies that in MVC-EMA the end-member matrix  $\mathbf{G}$ , instead of abundance matrix  $\mathbf{W}$ , tends to be sparse.

To derive the uniqueness of the solution of MVC-EMA (2), we need the following assumptions as in Fu et al. (2018, 2015); Leplat et al. (2020).

**Assumption A1:** The matrices  $\mathbf{W}$  and  $\mathbf{G}$  satisfy  $\text{rank}(\mathbf{W}) = \text{rank}(\mathbf{G}) = K$ .

**Assumption A2:**  $\mathbf{G} \in \mathbb{R}_+^{K \times J}$  is satisfied with sufficiently scattered conditions (SSC):

(1) SSC1:  $\mathbb{C} \subseteq \text{cone}(\mathbf{G})$ , where  $\mathbb{C} = \{\mathbf{x} \in \mathbb{R}_+^K | \mathbf{1}^T \mathbf{x} \geq \sqrt{K-1} \|\mathbf{x}\|_2\}$  is second-order cone;

(2) SSC2:  $\text{cone}^*(\mathbf{G}) \cap \text{bd}\mathbb{C}^* = \{\alpha \mathbf{e}_k | \alpha \geq 0, k = 1, \dots, K\}$ , where the dual of  $\mathbb{C}$  is defined as  $\mathbb{C}^* = \{\mathbf{x} \in \mathbb{R}^K | \mathbf{1}^T \mathbf{x} \geq \|\mathbf{x}\|_2\}$ .

We show that Assumptions A1 and A2 are a sufficient condition for the uniqueness of the solution of MVC-EMA.

**Theorem 1.** *Under Assumptions A1 and A2, MVC-EMA uniquely identifies  $\tilde{\mathbf{W}}$  and  $\tilde{\mathbf{G}}$  up to permutation, i.e., any optimal solution  $\mathbf{W}_\#$  and  $\mathbf{G}_\#$  to MVC-EMA (2) takes the form:*

$$\mathbf{W}_\# = \tilde{\mathbf{W}} \mathbf{U}^{-1} \text{ and } \mathbf{G}_\# = \mathbf{U} \tilde{\mathbf{G}} \quad (3)$$

where  $\mathbf{U}$  is a permutation matrix.

*Proof.* Step 1: Let us consider both  $(\tilde{\mathbf{W}}, \tilde{\mathbf{G}})$  and  $(\mathbf{W}_\#, \mathbf{G}_\#)$  to be optimal solutions for (2). Since  $\text{rank}(\tilde{\mathbf{W}}) = \text{rank}(\tilde{\mathbf{G}}) = \text{rank}(\mathbf{W}_\#) = \text{rank}(\mathbf{G}_\#) = K$ , there exists a full rank matrix  $\mathbf{U}$  of size  $K \times K$  such that

$$\mathbf{W}_\# = \tilde{\mathbf{W}} \mathbf{U}^{-1} \text{ and } \mathbf{G}_\# = \mathbf{U} \tilde{\mathbf{G}}.$$

The matrix  $\mathbf{U}$  has row-sum-to-1 constraint because

$$\mathbf{1} = \mathbf{G}_\# \mathbf{1} = \mathbf{U} \tilde{\mathbf{G}} \mathbf{1} = \mathbf{U} \mathbf{1} \quad (4)$$

Step 2: From  $\mathbf{G}_\# = \mathbf{U} \tilde{\mathbf{G}}$ , the vectors in rows of  $\mathbf{U}$  belong to dual cone of  $\tilde{\mathbf{G}}$ , i.e.,  $\mathbf{U}(i,:)^T \in \text{cone}^*(\tilde{\mathbf{G}})$  for  $i = 1, \dots, I$  where  $\mathbf{U}(i,:)$  is a row vector with elements being the  $i$ th row of  $\mathbf{U}$ . According to SSC1 ( $\mathbb{C} \subseteq \text{cone}(\tilde{\mathbf{G}})$ ), we have  $\text{cone}^*(\tilde{\mathbf{G}}) \subseteq \mathbb{C}^*$ . Thus,  $\mathbf{U}(i,:)^T \in \mathbb{C}^*$ . This means

$$\|\mathbf{U}(i,:)^T\|_2 \leq \mathbf{1}^T \mathbf{U}(i,:)^T \quad (5)$$

Therefore,

$$|\det(\mathbf{U})| = |\det(\mathbf{U}^T)| \leq \prod_i \|\mathbf{U}(i,:)^T\|_2 \leq \prod_i \mathbf{1}^T \mathbf{U}(i,:)^T = 1.$$

where the first inequality is the Hadamard's inequality, the second follows (5), the last equality follows (4).

Step 3: If  $|\det(\mathbf{U})| < 1$ , then

$$\det(\mathbf{G}_\# \mathbf{G}_\#^T) = \det(\mathbf{U} \tilde{\mathbf{G}} \tilde{\mathbf{G}}^T \mathbf{U}^T) = |\det(\mathbf{U})|^2 \det(\tilde{\mathbf{G}} \tilde{\mathbf{G}}^T) < \det(\tilde{\mathbf{G}} \tilde{\mathbf{G}}^T).$$

This means that  $\mathbf{G}_\#$  does not have the maximum volume, which is contradict with that  $(\mathbf{W}_\#, \mathbf{G}_\#)$  is an optimal solution.

Step 4: If  $|\det(\mathbf{U})| = 1$ , then all inequalities needs to be equalities. Hence, for all  $i$ ,  $\|\mathbf{U}(i, :)^T\|_2 = \mathbf{1}^T \mathbf{U}(i, :)^T$ , implying that  $\mathbf{U}(i, :)^T$  is the boundary of  $\mathbb{C}^*$ . And  $\mathbf{U}(i, :)^T \in \text{cone}^*(\tilde{\mathbf{G}})$ . According to SSC2, we have  $\mathbf{U}(i, :)^T = \alpha \mathbf{e}_k$ .

Step 5: And due to the constraint  $\mathbf{U}\mathbf{1} = \mathbf{1}$  in Equation (4), we have  $\alpha = 1$ . Thus  $\mathbf{U}$  can only be a permutation matrix.  $\square$

It is worth noting that the maximum volume assumption and the proof process of Theorem 1 are similar to the minimum volume assumption and the uniqueness theorem in minimum volume constrained NMF (Fu et al., 2018, 2015; Leplat et al., 2020), but the maximum volume assumption and Theorem 1 are novel, provide a new perspective, specifically for highly mixed data. Note that the SSC constraint holds for the basis matrix  $\mathbf{G}$  instead of coefficient matrix  $\mathbf{W}$ .

We provide an illustration for SSC using Figure 2 for  $K = 3$  (Gillis, 2020; Qi & Van der Heijden, 2025). Figure 2 assumes that viewer stands in the nonnegative orthant, faces the origin, and looks at the two-dimensional plane  $\mathbf{x}\mathbf{1} = \mathbf{1}$  (Gillis, 2020). Specifically, the dots "o" correspond to columns of  $\mathbf{G}$ ; the crosses "X" are standard basis vectors  $\mathbf{e}_1, \mathbf{e}_2, \mathbf{e}_3$ , the circle corresponds to the second-order cone  $\mathbb{C}$ ; the triangle corresponds to nonnegative orthant cone( $\mathbf{e}_1, \mathbf{e}_2, \mathbf{e}_3$ ); the polygon is  $\text{cone}(\mathbf{G})$ . The circle is contained in the polygon. I.e., SSC1 holds.

Geometrically, SSC2 means that the only orthogonal matrix  $\mathbf{Q}$  such that  $\text{cone}(\mathbf{G}) \subseteq \text{cone}(\mathbf{Q})$  is a permutation matrix (Gillis, 2020). The cone generated by the columns of any permutation matrix is exactly the triangle in the figure. Any orthogonal matrix is a rotated version of the triangle in the figure. As shown in the figure, the rotated version of the nonnegative orthant cone( $\mathbf{e}_1, \mathbf{e}_2, \mathbf{e}_3$ ) (except for itself) does not contain the polygon formed by the dots. Thus, SSC2 hold.

In Figure 2, some column points in  $\mathbf{G}$  are located on the edge of the triangle, implying there is a zero element in these columns. Thus, the end-member matrix  $\mathbf{G}$  is sparse. In contrast, in minimum volume constrained NMF, the abundance matrix  $\mathbf{W}$  is satisfied with SSC, and thus the abundance matrix  $\mathbf{W}$  is sparse.

Next, we provide a quadratic programming algorithm for MVC-EMA, inspired by the NMF literature (Gillis, 2014, 2020; Leplat, Ang, & Gillis, 2019; Zhou, Xie, Yang, Yang, & He, 2011).

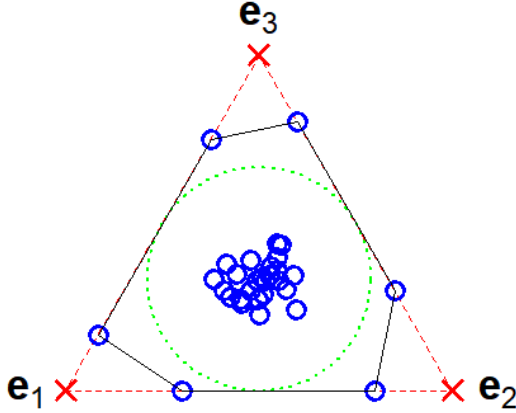


Figure 2: Geometric illustrations that end-member matrix  $\mathbf{G}$  satisfies SSC.

### 3 APFGM algorithm

In this paper, we consider MVC-EMA in which the observed data matrix  $\mathbf{P}$  is approximated by  $\mathbf{\Pi} = \mathbf{W}\mathbf{G}$ . The approximation error, quantified by the squared Frobenius norm  $\|\mathbf{P} - \mathbf{W}\mathbf{G}\|_F^2$ , serves as the data fitting term, while  $\det(\mathbf{G}\mathbf{G}^T)$  acts as a volume regularizer. The resulting objective function for MVC-EMA is given by

$$\begin{aligned} \min_{\mathbf{W}, \mathbf{G}} \quad & J(\mathbf{W}, \mathbf{G}) = \frac{1}{2} \|\mathbf{P} - \mathbf{W}\mathbf{G}\|_F^2 - \frac{\lambda}{2} \det(\mathbf{G}\mathbf{G}^T) \\ \text{subject to} \quad & \mathbf{W}\mathbf{1} = \mathbf{1}, \quad \mathbf{G}\mathbf{1} = \mathbf{1}, \quad \mathbf{W} \in \mathbb{R}_+^{I \times K}, \quad \mathbf{G} \in \mathbb{R}_+^{K \times J}. \end{aligned} \quad (6)$$

The regularization parameter  $\lambda \geq 0$  controls the tradeoff between the data fitting term  $\|\mathbf{P} - \mathbf{W}\mathbf{G}\|_F^2$  and the volume regularizer  $\det(\mathbf{G}\mathbf{G}^T)$ . Because of the negative sign before  $\lambda$ , increasing  $\lambda$  results in an increase in the volume. This negative sign is a crucial difference between MVC-EMA and minimum volume constrained NMF, where the sign before  $\lambda$  is positive (Zhou et al., 2011).

For (6), simultaneously optimizing  $\mathbf{W}$  and  $\mathbf{G}$  is a non-convex problem. As in most work in NMF, we minimize the objective function alternatively over  $\mathbf{W}$  or  $\mathbf{G}$ , each time optimizing over one matrix while keeping the other one fixed. The iteration scheme of alternative optimization can be written as:

$$\mathbf{W} = \arg \min_{\mathbf{W}: \mathbf{W}\mathbf{1}=\mathbf{1}, \mathbf{W} \geq 0} J(\mathbf{W}, \mathbf{G}) \quad (7a)$$

$$\mathbf{G} = \arg \min_{\mathbf{G}: \mathbf{G}\mathbf{1}=\mathbf{1}, \mathbf{G} \geq 0} J(\mathbf{W}, \mathbf{G}) \quad (7b)$$

### 3.1 Updating the abundance matrix $\mathbf{W}$

In Equation (7a)  $\mathbf{G}$  is considered known. Given the known  $\mathbf{G}$ , the problem of Equation (7a) becomes  $\mathbf{W} = \arg \min_{\mathbf{W}: \mathbf{W} \mathbf{1} = \mathbf{1}, \mathbf{W} \geq 0} \frac{1}{2} \|\mathbf{P} - \mathbf{W}\mathbf{G}\|_F^2$  and is therefore a convex optimization problem (Gillis, 2020). Solving  $\min_{\mathbf{W}: \mathbf{W} \mathbf{1} = \mathbf{1}, \mathbf{W} \geq 0} \frac{1}{2} \|\mathbf{P} - \mathbf{W}\mathbf{G}\|_F^2$  is equivalent to solving subproblem

$$\begin{aligned} \min_{\mathbf{W}(i,:)} \quad & \frac{1}{2} \|\mathbf{P}(i,:) - \mathbf{W}(i,:)\mathbf{G}\|_F^2 \\ \text{subject to} \quad & \mathbf{W}(i,:)\mathbf{1} = \mathbf{1}, \mathbf{W}(i,:) \geq 0 \end{aligned} \quad (8)$$

for  $i = 1, \dots, I$ , where  $\mathbf{P}(i,:)$  or  $\mathbf{W}(i,:)$  is a row vector with elements being the  $i$ th row of  $\mathbf{P}$  or  $\mathbf{W}$ . For each  $i$ , it is equivalent to solving

$$\begin{aligned} \min_{\mathbf{W}(i,:)} \quad & \mathbf{W}(i,:) \left( \frac{1}{2} \mathbf{G}\mathbf{G}^T \right) \mathbf{W}(i,:)^T - \mathbf{P}(i,:)\mathbf{G}^T \mathbf{W}(i,:)^T \\ \text{subject to} \quad & \mathbf{W}(i,:)\mathbf{1} = \mathbf{1}, \mathbf{W}(i,:) \geq 0 \end{aligned} \quad (9)$$

which is a quadratic programming problem with nonnegative and row-sum-to-one constraints. In practice, the  $I$  subproblems can be solved in parallel. If the rank of  $\mathbf{G}$  is  $K$ ,  $\frac{1}{2} \mathbf{G}\mathbf{G}^T$  is positive definite. Thus, problem (9) can be solved by quadratic programming algorithm and the solution is unique (Zhou et al., 2011). Here, for updating  $\mathbf{W}(i,:)$ , following Gillis (2014); Leplat et al. (2019), we use a projected fast gradient method (PFGM) (Nesterov, 2004).

### 3.2 Updating the end-member matrix $\mathbf{G}$

In Equation (7b)  $\mathbf{W}$  is a known matrix. As in updating abundance matrix, we express the objective function of Equation (7b) as  $K$  subproblems where each one is a quadratic programming problem.

Data fitting term  $\|\mathbf{P} - \mathbf{W}\mathbf{G}\|_F^2$  can be expressed as (Zhou et al., 2011)

$$\begin{aligned} \|\mathbf{P} - \mathbf{W}\mathbf{G}\|_F^2 &= \|\mathbf{P} - \sum_{l=1}^K \mathbf{W}(:,l)\mathbf{G}(l,:)\|_F^2 \\ &= \|\mathbf{P} - \sum_{l \neq k} \mathbf{W}(:,l)\mathbf{G}(l,:) - \mathbf{W}(:,k)\mathbf{G}(k,:)\|_F^2 \\ &= \|\mathbf{P}_k - \mathbf{W}(:,k)\mathbf{G}(k,:)\|_F^2 \\ &= \|\mathbf{P}_k\|_F^2 + \|\mathbf{W}(:,k)\|_F^2 \|\mathbf{G}(k,:)\|_F^2 - 2\mathbf{G}(k,:)\mathbf{P}_k^T \mathbf{W}(:,k) \end{aligned} \quad (10)$$

where  $\mathbf{W}(:,k)$  is a column vector with elements being the  $k$ th column of  $\mathbf{W}$  and  $\mathbf{G}(k,:)$  is a row vector with elements being the  $k$ th row of  $\mathbf{G}$ , and  $\mathbf{P}_k = \mathbf{P} - \sum_{l \neq k} \mathbf{W}(:,l)\mathbf{G}(l,:)$ .

Let  $\bar{\mathbf{G}}_k$  be the submatrix of  $\mathbf{G}$  by removing the  $k$ th row of  $\mathbf{G}$ . Then  $\mathbf{G} = \Gamma \begin{bmatrix} \mathbf{G}(k,:) \\ \bar{\mathbf{G}}_k \end{bmatrix}$

where  $\Gamma$  is a permutation matrix. Thus we have

$$\begin{aligned}
\det(\mathbf{G}\mathbf{G}^T) &= \det \left( \begin{bmatrix} \mathbf{G}(k,:) \\ \bar{\mathbf{G}}_k \end{bmatrix} \begin{bmatrix} \mathbf{G}(k,:) \\ \bar{\mathbf{G}}_k \end{bmatrix}^T \right) \\
&= \det \left( \begin{bmatrix} \mathbf{G}(k,:) \\ \bar{\mathbf{G}}_k \end{bmatrix} \left[ \mathbf{G}(k,:)^T, \bar{\mathbf{G}}_k^T \right] \right) \\
&= \det \left( \bar{\mathbf{G}}_k \bar{\mathbf{G}}_k^T \right) \det \left( \mathbf{G}(k,:)(\mathbf{I} - \bar{\mathbf{G}}_k^T (\bar{\mathbf{G}}_k \bar{\mathbf{G}}_k^T)^{-1} \bar{\mathbf{G}}_k) \mathbf{G}(k,:)^T \right) \\
&= \det \left( \bar{\mathbf{G}}_k \bar{\mathbf{G}}_k^T \right) \left( \mathbf{G}(k,:)(\mathbf{I} - \bar{\mathbf{G}}_k^T (\bar{\mathbf{G}}_k \bar{\mathbf{G}}_k^T)^{-1} \bar{\mathbf{G}}_k) \mathbf{G}(k,:)^T \right).
\end{aligned} \tag{11}$$

The last equality holds because  $\left( \mathbf{G}(k,:)(\mathbf{I} - \bar{\mathbf{G}}_k^T (\bar{\mathbf{G}}_k \bar{\mathbf{G}}_k^T)^{-1} \bar{\mathbf{G}}_k) \mathbf{G}(k,:)^T \right)$  is a matrix of size  $1 \times 1$ . We have

$$\mathbf{G}(k,:)(\mathbf{I} - \bar{\mathbf{G}}_k^T (\bar{\mathbf{G}}_k \bar{\mathbf{G}}_k^T)^{-1} \bar{\mathbf{G}}_k) \mathbf{G}(k,:)^T = \mathbf{G}(k,:)\mathbf{C}_k \mathbf{C}_k^T \mathbf{G}(k,:)^T \tag{12}$$

where  $\mathbf{C}_k = \text{Null}(\bar{\mathbf{G}}_k)$  is an orthonormal basis for the null space of  $\bar{\mathbf{G}}_k$ . The reason can be seen as follows. From  $\mathbf{C}_k = \text{Null}(\bar{\mathbf{G}}_k)$ , we have  $\mathbf{C}_k^T \mathbf{C}_k = \mathbf{I}$  and  $\bar{\mathbf{G}}_k \mathbf{C}_k = \mathbf{0}$ . The column of  $\mathbf{C}_k$  and the rows of  $\bar{\mathbf{G}}_k$  together form a base of the  $J$ -dimensional space. Therefore, any vector  $\mathbf{G}(k,:)^T$  can be expressed as  $\mathbf{G}(k,:)^T = \mathbf{C}_k \mathbf{x} + \bar{\mathbf{G}}_k^T \mathbf{y}$ . Then we have

$$\mathbf{G}(k,:)\mathbf{G}(k,:)^T = \mathbf{x}^T \mathbf{x} + \mathbf{y}^T \bar{\mathbf{G}}_k \bar{\mathbf{G}}_k^T \mathbf{y}.$$

Note that  $\bar{\mathbf{G}}_k \mathbf{G}(k,:)^T = \bar{\mathbf{G}}_k \bar{\mathbf{G}}_k^T \mathbf{y}$ . Therefore,  $\mathbf{G}(k,:)\bar{\mathbf{G}}_k^T (\bar{\mathbf{G}}_k \bar{\mathbf{G}}_k^T)^{-1} \bar{\mathbf{G}}_k \mathbf{G}(k,:)^T = \mathbf{y}^T \bar{\mathbf{G}}_k \bar{\mathbf{G}}_k^T \mathbf{y}$ . Note that  $\mathbf{C}_k^T \mathbf{G}(k,:)^T = \mathbf{x}$ . Hence,  $\mathbf{x}^T \mathbf{x} = \mathbf{G}(k,:)\mathbf{C}_k \mathbf{C}_k^T \mathbf{G}(k,:)^T$ . Therefore,

$$\mathbf{G}(k,:)\mathbf{G}(k,:)^T - \mathbf{G}(k,:)\bar{\mathbf{G}}_k^T (\bar{\mathbf{G}}_k \bar{\mathbf{G}}_k^T)^{-1} \bar{\mathbf{G}}_k \mathbf{G}(k,:)^T = \mathbf{x}^T \mathbf{x} = \mathbf{G}(k,:)\mathbf{C}_k \mathbf{C}_k^T \mathbf{G}(k,:)^T.$$

The proof for Equation (12) is completed. Combined Equation (11) with Equation (12), volume term  $\det(\mathbf{G}\mathbf{G}^T)$  can be expressed as

$$\det(\mathbf{G}\mathbf{G}^T) = \det(\bar{\mathbf{G}}_k \bar{\mathbf{G}}_k^T) \mathbf{G}(k,:)\mathbf{C}_k \mathbf{C}_k^T \mathbf{G}(k,:)^T \tag{13}$$

Combined Equation (10) with Equation (13), the problem of Equation (7b) is decomposed into  $K$  independent sub-problems which are quadratic programming problems:

$$\begin{aligned}
\min_{\mathbf{G}(k,:)} \quad & \mathbf{G}(k,:)\mathbf{Q}_k \mathbf{G}(k,:)^T - \mathbf{W}(:,k)^T \mathbf{P}_k \mathbf{G}(k,:)^T \\
\text{subject to} \quad & \mathbf{G}(k,:)\mathbf{1} = \mathbf{1}, \mathbf{G}(k,:)^T \geq 0
\end{aligned} \tag{14}$$

where  $\mathbf{Q}_k = \frac{1}{2} \mathbf{W}(:,k)^T \mathbf{W}(:,k) \mathbf{I} - \frac{\lambda}{2} \det(\bar{\mathbf{G}}_k \bar{\mathbf{G}}_k^T) \mathbf{C}_k \mathbf{C}_k^T$  and  $\mathbf{P}_k = \mathbf{P} - \sum_{l \neq k} \mathbf{W}(:,l) \mathbf{G}(l,:)$ . In practice, the subproblems are solved alternatively where  $\mathbf{Q}_k$  and  $\mathbf{P}_k$  use the latest rows of  $\mathbf{G}$ . The strict convexity of Equation (14) requires  $\mathbf{Q}_k$  to be positive definite. Consequently, the value of  $\lambda$  cannot be too large. Again, following Gillis (2014); Leplat et al. (2019), we use PFGM on Equation (14) (Nesterov, 2004).

We call this algorithm APFGM, short for alternative projected fast gradient methods. See algorithm 1 for a conclusion, where  $\lambda$  in (6) is computed by scaling the input  $\lambda'$ :  $\lambda = \lambda' \frac{\|P - W^{(0)}G^{(0)}\|_F^2}{\det(G^{(0)}(G^{(0)})^T)}$ , with  $W^{(0)}$  and  $G^{(0)}$  being the initial input matrices.

Note that, in APFGM,  $\lambda$  can be negative, where APFGM tends to obtain basis vectors as closely as possible, which follows the minimum volume assumption (Zhou et al., 2011).

---

**Algorithm 1:** Alternative projected fast gradient methods (APFGM)

---

**Input:** Input nonnegative matrix  $P \in \mathbb{R}_+^{I \times J}$  with row-sum-to-one constraint

$P\mathbf{1} = \mathbf{1}$ , dimensionality  $K$ , number of iterations maxiter, and  $\lambda'$ .

**Output:**  $W \geq 0$  with  $W\mathbf{1} = \mathbf{1}$  and  $G \geq 0$  with  $G\mathbf{1} = \mathbf{1}$ .

Generate initial matrices  $W^{(0)} \geq 0$  with  $W^{(0)}\mathbf{1} = \mathbf{1}$  and  $G^{(0)} \geq 0$  with  $G^{(0)}\mathbf{1} = \mathbf{1}$ .

Let  $\lambda = \lambda' \frac{\|P - W^{(0)}G^{(0)}\|_F^2}{\det(G^{(0)}(G^{(0)})^T)}$ .

**for**  $t = 1, 2, \dots, \text{maxiter}$  **do**

    Apply FPGD to the quadratic programming problem Equation (9) to update abundance matrix  $W$

    Apply FPGD to the quadratic programming problem Equation (14) to update end-member matrix  $G$

---

### 3.3 Applying APFGM to the simulated GSD data in the Introduction

We perform APFGM on the same simulated GSD data as in the Introduction. When  $\lambda < 0$ , i.e., minimum volume constraint, the results in Figures 3a and 3b are similar to Figures 1c and 1d from EMMA, and cannot obtain the true EMs and misestimate abundances. We find the same results in Figures 3c and 3d for  $\lambda = 0$ , i.e., no volume constraint. However, when  $\lambda > 0$ , i.e., using the maximum volume assumption, APFGM recovers the true EMs and abundances; see Figures 3e and 3f. The determinant of  $GG^T$  for APFGM with minimum volume, APFGM with no volume, and EMMA is around 0.0015, but for APFGM with maximum volume is around 0.0028. APFGM with maximum volume tends to find end members as different as possible which makes it suitable for this highly mixed GSD data.

## 4 Experiments

In this section, we simulate different levels of mixing GSD data to extensively explore the performance of APFGM. The code for this paper is available on the Github website <https://github.com/qianqianqi28/MVC-EMA>, implemented in MATLAB R2024b and R 4.2.3.

### 4.1 Generation of artificial GSD data

Three end members (EMs), simulated by lognormal distributions, are presented in Figure 4 where each EMs have 100 values. Six artificial GSD data are then produced by combining these EMs with random abundances where each GDS data have 200 specimen, and the

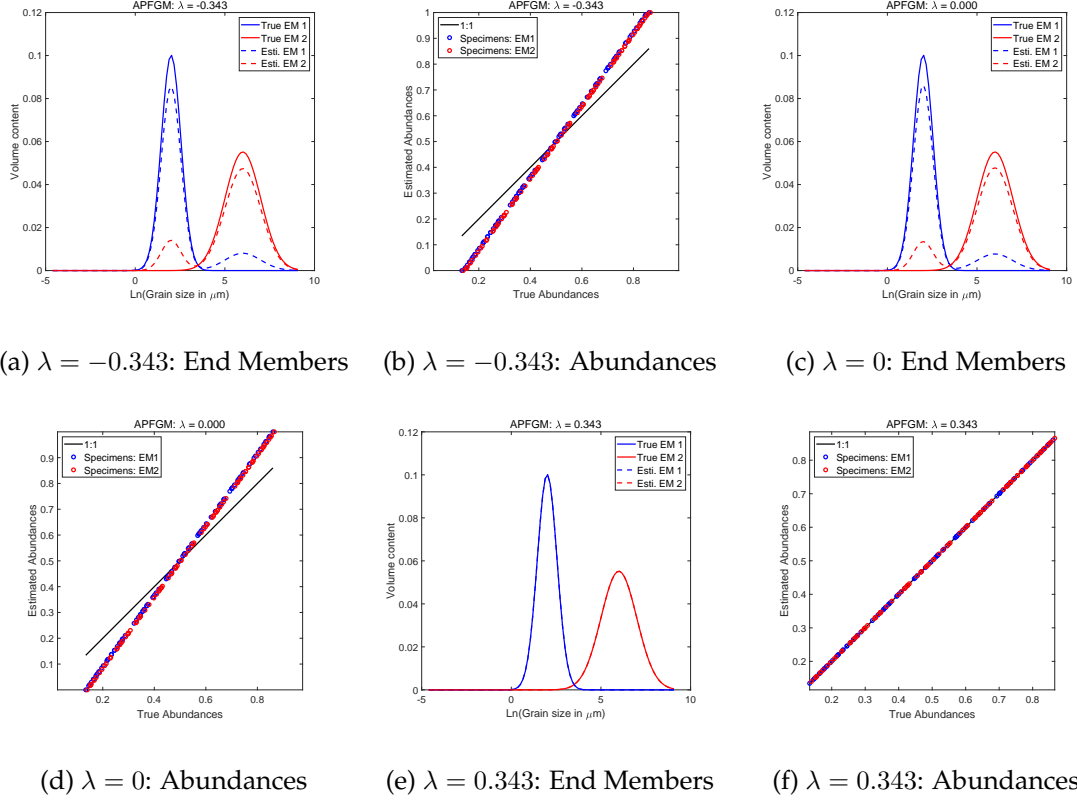


Figure 3: APFGM: (a and b)  $\lambda = -0.343$ ; (c and d)  $\lambda = 0$ ; (e and f)  $\lambda = 0.343$ .

minimum abundance for each specimen was varied from 0 to 0.25 in increments of 0.05 to simulate conditions ranging from poorly mixed to highly mixed, respectively.

#### 4.2 Indexes used to evaluate the unmixing results

We use mean angular deviations (in degrees) between true EMs and estimated EMs to evaluate estimated GSDs:

$$\text{MAEM} = \frac{180}{\pi K} \sum_{k=1}^K \arccos \left( \frac{\langle \text{True } \mathbf{G}(k, :) \rangle, \text{Est. } \mathbf{G}(k, :) \rangle}{\|\text{True } \mathbf{G}(k, :)\| \|\text{Est. } \mathbf{G}(k, :)\|} \right) \quad (15)$$

and use mean angular deviations (in degrees) between true abundances and estimated abundances to evaluate estimated abundances:

$$\text{MAAB} = \frac{180}{\pi I} \sum_{i=1}^I \arccos \left( \frac{\langle \text{True } \mathbf{W}(i, :) \rangle, \text{Est. } \mathbf{W}(i, :) \rangle}{\|\text{True } \mathbf{W}(i, :)\| \|\text{Est. } \mathbf{W}(i, :)\|} \right) \quad (16)$$

The range of MAEM and MAAB is larger or equal to 0 degrees and less or equal to 90 degrees. The smaller MAEM or EAAB is, the better an algorithm is. MAEM (MAAB) with a value of 0 means that estimated EMs (abundances) are identical to true EMs (abundances). MAEM (MAAB) with a value of 90 means that estimated EMs (abundances) are orthogonal to true EMs (abundances).

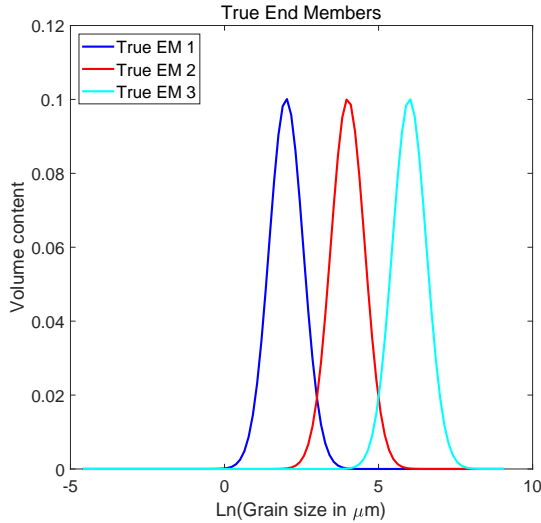


Figure 4: Three lognormal EMs.

#### 4.3 Comparison of EMMA, APFGM with minimum volume, APFGM with no volume, and APFGM with maximum volume

The scaling factor  $\lambda'$  controls the volume regularization in APFGM. It is set to  $-1, 0, 1$  for APFGM with minimum volume, with no volume, and with maximum volume, respectively. The MAEM and MAAB against increasing degree of mixing are plotted in Figure 5a and Figure 5b respectively and are shown in Table 1 and Table 2 respectively. We can see that APFGM with maximum volume is best, then APFGM with no volume, finally, EMMA and APFGM with minimum volume. Specifically, at zero level, APFGM with no volume and APFGM with maximum volume estimate the true end-members and abundances more accurately than EMMA and APFGM with minimum volume. This means that APFGM algorithm is also suitable for no mixed GSD data. As level of mixing increases, EMMA and APFGM with no volume and minimum volume cannot clearly estimate EMs and abundances, but APFGM with maximum volume fits the true EMs and abundances, with a slight deterioration. This highlights the usefulness of maximum volume regularizer in highly mixed data sets.

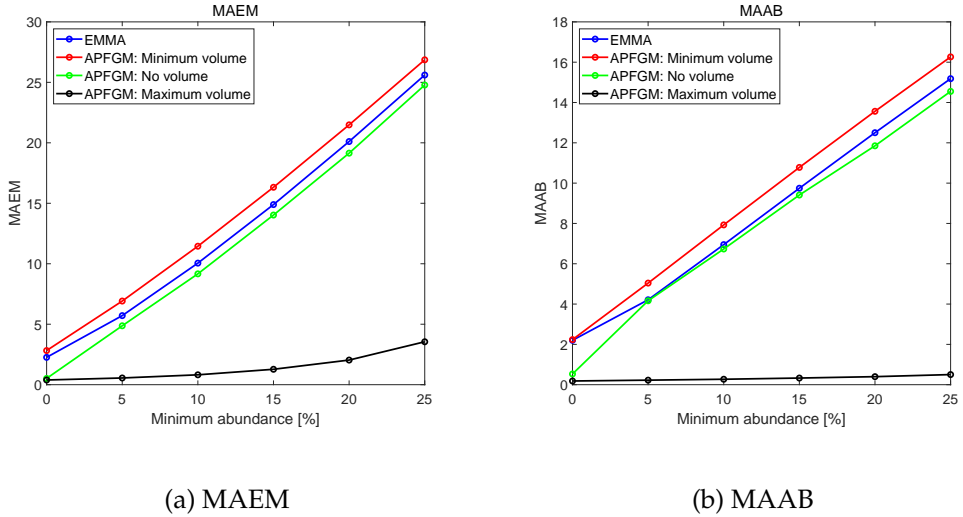


Figure 5: EMMA, APFGM with minimum volume, APFGM with no volume, and APFGM with maximum volume: (a) MAEM; (b) MAAB.

Table 1: The MAEM of EMMA, APFGM with minimum volume, APFGM with no volume, and APFGM with maximum volume under different mixed level.

Mixed level	EMMA	APFGM min	APFGM no	APFGM max
0.00	2.2602	2.8223	0.5175	0.3883
0.05	5.7117	6.9162	4.8707	0.5551
0.10	10.0522	11.4498	9.1652	0.8163
0.15	14.8928	16.3239	14.0272	1.2743
0.20	20.1057	21.4845	19.1438	2.0358
0.25	25.6058	26.8632	24.7793	3.5488

Table 2: The MAAB of EMMA, APFGM with minimum volume, APFGM with no volume, and APFGM with maximum volume under different mixed level.

Mixed level	EMMA	APFGM min	APFGM no	APFGM max
0.00	2.2020	2.2359	0.5307	0.1834
0.05	4.2121	5.0408	4.1633	0.2248
0.10	6.9495	7.9277	6.7321	0.2700
0.15	9.7462	10.7792	9.4098	0.3296
0.20	12.5014	13.5635	11.8517	0.3982
0.25	15.1823	16.2625	14.5505	0.5017

Figure 6 shows the end-members and abundances for a minimum abundance of 15%. The estimated end-members from EMMA and APFGM with  $\lambda \leq 0$  exhibit contamination with each other of three EMs and leading to mis-estimated abundances, but APFGM with maximum volume better recover the unimodal sources. Thus, APFGM with maximum

volume exhibits a resistant for highly mixed GSD data.

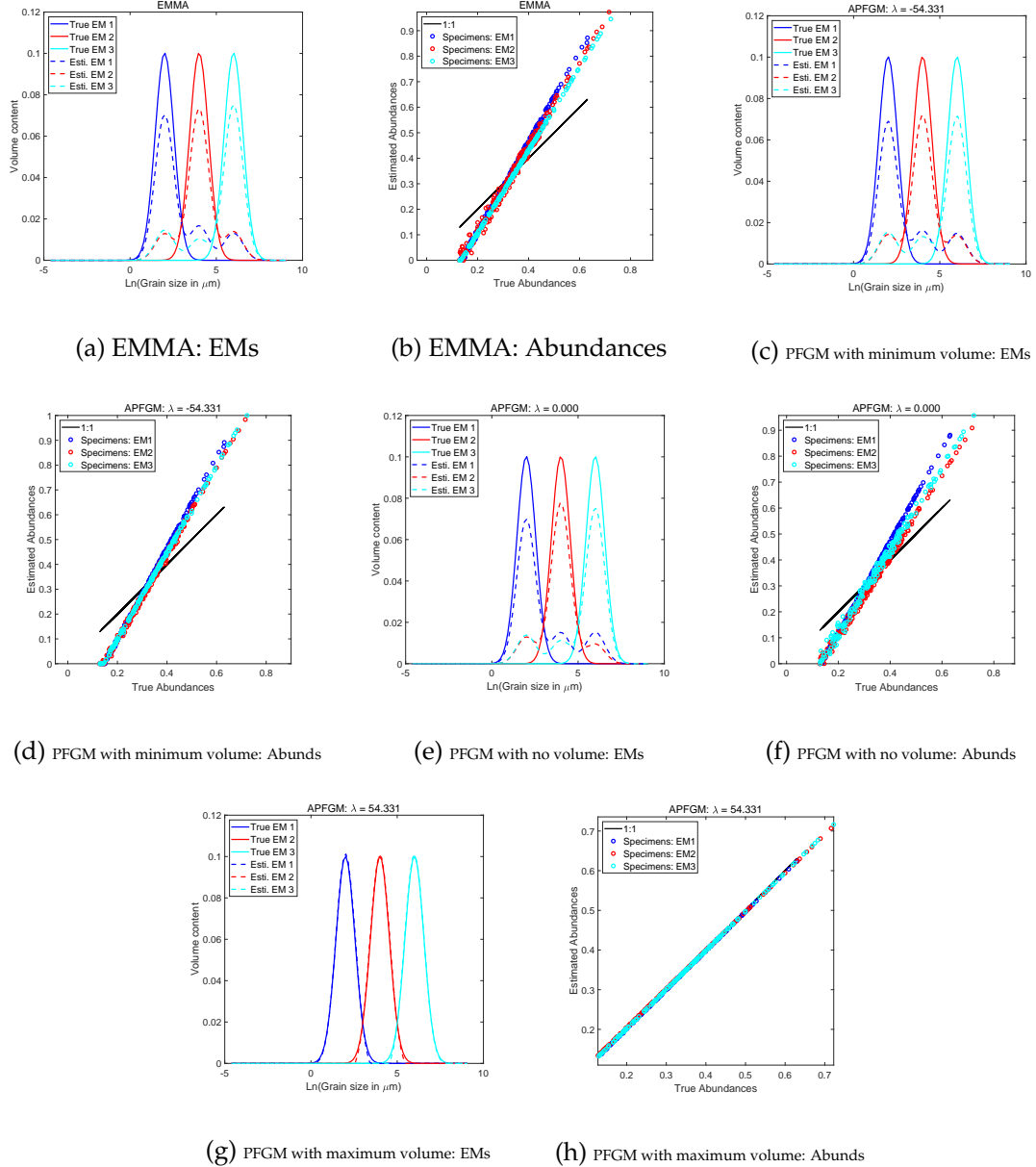


Figure 6: (a and b) EMMA; (c and d) PFGM with minimum volume; (e and f) PFGM with no volume; (g and h) PFGM with maximum volume.

The volume  $\det(\mathbf{G}\mathbf{G}^T)$  against increasing degree of mixing is shown in Figure 7 and Table 3. We can see that APFGM with maximum volume has maximum volume, APFGM with no volume is second, and finally, EMMA and APFGM with minimum volume for any level of mixing. As increasing the level of mixing, the volume  $\det(\mathbf{G}\mathbf{G}^T)$  increases for APFGM with maximum volume and decreases for EMMA and APFGM with no volume and minimum volume.

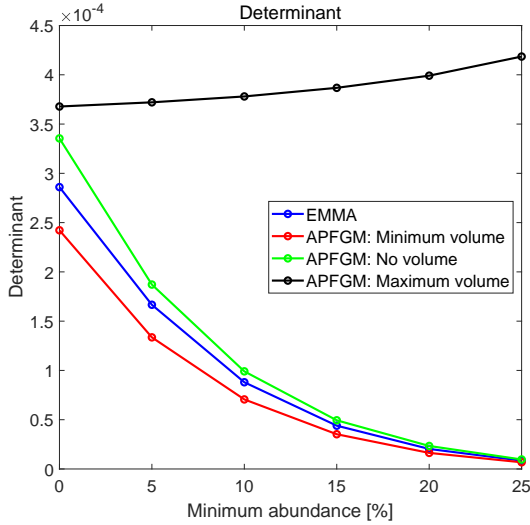


Figure 7: EMMA, APFGM with minimum volume, APFGM with no volume, and APFGM with maximum volume:  $\det(\mathbf{G}\mathbf{G}^T)$ .

Table 3: The  $\det(\mathbf{G}\mathbf{G}^T)$  of EMMA, APFGM with minimum volume, APFGM with no volume, and APFGM with maximum volume under different mixed level.

Mixed level	EMMA	APFGM min	APFGM no	APFGM max
0.00	0.2860	0.2422	0.3355	0.3678
0.05	0.1666	0.1336	0.1871	0.3721
0.10	0.0880	0.0706	0.0991	0.3780
0.15	0.0439	0.0353	0.0494	0.3868
0.20	0.0203	0.0163	0.0234	0.3991
0.25	0.0085	0.0068	0.0096	0.4185

## 5 Conclusion

To conclude, in this paper, we propose maximum volume constrained EMA (MVC-EMA) for highly mixed GSD data. We prove that MVC-EMA is unique under the sufficient scattered conditions, a new NMF identification criterion that is careful tweak of the existing volume minimization criterion in minimum volume constrained NMF. We introduce APFGM which makes use of alternative projected fast gradient methods. Experimental results show that APFGM with maximum volume can effective deal with highly mixed GSD data than APFGM with minimum volume, APFGM with no volume, and EMMA. However, as a new method, there are still some important issues that are in need of further research. First, MVC-EMA needs to be tested on some real SGD to fully evaluate its performance. Second, algorithms which allows the balancing parameter to be any number need to be investigated.

## Acknowledgments

Zhongming Chen is partially supported by Natural Science Foundation of Zhejiang Province (No. LY22A010012) and Natural Science Foundation of Xinjiang Uygur Autonomous Region (No. 2024D01A09).

## Competing Interests

No potential competing interest was reported by the authors.

## References

Abdolali, M., Barbarino, G., & Gillis, N. (2024). Dual simplex volume maximization for simplex-structured matrix factorization. *SIAM Journal on Imaging Sciences*, 17(4), 2362-2391.

Avis, D., & Bremner, D. (1995). How good are convex hull algorithms? In *Proceedings of the eleventh annual symposium on computational geometry* (p. 20-28). New York, NY, USA: Association for Computing Machinery.

Clogg, C. C. (1981). Latent structure models of mobility. *American Journal of Sociology*, 86(4), 836-868.

De Leeuw, J., Van der Heijden, P. G. M., & Verboon, P. (1990). A latent time-budget model. *Statistica Neerlandica*, 44(1), 1-22.

Dietze, M., Schulte, P., & Dietze, E. (2022). Application of end-member modelling to grain-size data: Constraints and limitations. *Sedimentology*, 69(2), 845-863.

Fu, X., Huang, K., & Sidiropoulos, N. D. (2018). On identifiability of nonnegative matrix factorization. *IEEE Signal Processing Letters*, 25(3), 328-332.

Fu, X., Huang, K., Sidiropoulos, N. D., & Ma, W.-K. (2019). Nonnegative matrix factorization for signal and data analytics: Identifiability, algorithms, and applications. *IEEE Signal Processing Magazine*, 36(2), 59-80.

Fu, X., Huang, K., Yang, B., Ma, W.-K., & Sidiropoulos, N. D. (2016). Robust volume minimization-based matrix factorization for remote sensing and document clustering. *IEEE Transactions on Signal Processing*, 64(23), 6254-6268.

Fu, X., Ma, W.-K., Huang, K., & Sidiropoulos, N. D. (2015). Blind separation of quasi-stationary sources: Exploiting convex geometry in covariance domain. *IEEE Transactions on Signal Processing*, 63(9), 2306-2320.

Gillis, N. (2014). Successive nonnegative projection algorithm for robust nonnegative blind source separation. *SIAM Journal on Imaging Sciences*, 7(2), 1420-1450.

Gillis, N. (2020). *Nonnegative matrix factorization*. Philadelphia, PA: Society for Industrial and Applied Mathematics.

Guo, Y.-T., Li, Q.-Q., & Liang, C.-S. (2024). The rise of nonnegative matrix factorization: Algorithms and applications. *Information Systems*, 123, 102379.

Hobolth, A., Guo, Q., Kousholt, A., & Jensen, J. L. (2020). A unifying framework and comparison of algorithms for non-negative matrix factorisation. *International Statistical Review*, 88(1), 29–53.

Jelihovschi, E., & Allaman, I. B. (2018). lba: An r package for latent budget analysis. *The R Journal*, 10, 269-287.

Lee, D. D., & Seung, H. S. (1999). Learning the parts of objects by non-negative matrix factorization. *Nature*, 401(6755), 788-791.

Leplat, V., Ang, A. M., & Gillis, N. (2019). Minimum-volume rank-deficient nonnegative matrix factorizations. In *Icassp 2019 - 2019 ieee international conference on acoustics, speech and signal processing (icassp)* (p. 3402-3406).

Leplat, V., Gillis, N., & Ang, A. M. (2020). Blind audio source separation with minimum-volume beta-divergence NMF. *IEEE Transactions on Signal Processing*, 68, 3400-3410.

Lin, C.-H., Ma, W.-K., Li, W.-C., Chi, C.-Y., & Ambikapathi, A. (2015). Identifiability of the simplex volume minimization criterion for blind hyperspectral unmixing: The no-pure-pixel case. *IEEE Transactions on Geoscience and Remote Sensing*, 53(10), 5530-5546.

Lin, Z., Wan, Q., Zhang, F., Zhong, J., Zhou, Z., & Bao, K. (2025). Using end-member model algorithm to infer sedimentary processes from mangrove sediment grain-size in guangdong, south china. *Regional Studies in Marine Science*, 83, 104069.

Liu, Y., Wang, T., Liu, B., Long, Y., Liu, X., & Sun, Y. (2023). Universal decomposition model: An efficient technique for palaeoenvironmental reconstruction from grain-size distributions. *Sedimentology*, 70(7), 2127-2149.

Moskalewicz, D., & Winter, C. (2024). Identification of sandy nourished sediments using end-member analysis (emmageo) applied to particle shapes distributions, sylt island, north sea. *Marine Geology*, 467, 107201.

Nesterov, Y. (2004). *Introductory lectures on convex optimization: A basic course*. Springer New York, NY.

Paatero, P., & Tapper, U. (1994). Positive matrix factorization: A non-negative factor model with optimal utilization of error estimates of data values. *Environmetrics*, 5(2), 111-126.

Paterson, G. A., & Heslop, D. (2015). New methods for unmixing sediment grain size data. *Geochemistry, Geophysics, Geosystems*, 16(12), 4494-4506.

Qi, Q., & Van der Heijden, P. G. M. (2025). *A review of NMF, PLSA, LBA, EMA, and LCA with a focus on the identifiability issue*. arXiv: 2512.22282.

Renner, R. M. (1993). The resolution of a compositional data set into mixtures of fixed source compositions. *Journal of the Royal Statistical Society Series C: Applied Statistics*, 42(4), 615-631.

Renner, R. M. (1995). The construction of extreme compositions. *Mathematical Geology*, 27(4), 485-497.

Renny, A., Kawsar, M., Manoj, M., Bikkina, S., Phartiyal, B., Kurian, P. J., ... Thakur, B. (2026). Decoding the sedimentary responses to the monsoon seasonality and ocean

circulation in the southeast arabian sea during the last 50 ka. *Palaeogeography, Palaeoclimatology, Palaeoecology*, 681, 113384.

Saberi-Movahed, F., Berahmand, K., Sheikhpour, R., Li, Y., Pan, S., & Jalili, M. (2025). Non-negative matrix factorization in dimensionality reduction: A survey. *ACM Computing Surveys*, 58(5).

Seidel, M., & Hlawitschka, M. (2015). An R-based function for modeling of end member compositions. *Mathematical Geosciences*, 47(8), 995-1007.

Van Hateren, J., Prins, M., & Van Balen, R. (2018). On the genetically meaningful decomposition of grain-size distributions: A comparison of different end-member modelling algorithms. *Sedimentary Geology*, 375, 49-71. (Analysis of sediment properties)

Van der Ark, L. A., Van der Heijden, P. G. M., & Sikkel, D. (1999). On the identifiability in the latent budget model. *Journal of Classification*, 16(1), 117-137.

Van der Heijden, P. G. M. (1994). End-member analysis and latent budget analysis. *Journal of the Royal Statistical Society Series C: Applied Statistics*, 43(3), 527-530.

Weltje, G. J. (1997). End-member modeling of compositional data: Numerical-statistical algorithms for solving the explicit mixing problem. *Mathematical Geology*, 29(4), 503-549.

Weltje, G. J., & Prins, M. A. (2007). Genetically meaningful decomposition of grain-size distributions. *Sedimentary Geology*, 202(3), 409-424. (From Particle Size to Sediment Dynamics)

Zhang, X., Wang, H., Xu, S., & Yang, Z. (2020). A basic end-member model algorithm for grain-size data of marine sediments. *Estuarine, Coastal and Shelf Science*, 236, 106656.

Zhou, G., Xie, S., Yang, Z., Yang, J.-M., & He, Z. (2011). Minimum-volume-constrained nonnegative matrix factorization: Enhanced ability of learning parts. *IEEE Transactions on Neural Networks*, 22(10), 1626-1637.